# Production and Measurements of Isolated Single-Wall Carbon Nanotubes

Sivaram Arepalli*, Pavel Nikolaev*, William Holmes*,
Victor Hadjiev[¶], and Bradley Files[$]

[*] *G. B. Tech./NASA-Johnson Space Center, 2101 NASA Road One, Houston, TX 77058, USA*
[¶] *Texas Center for Superconductivity, University of Houston, Houston, TX 77204, USA*
[$] *NASA-Johnson Space Center, 2101 NASA Road One, Houston, TX 77058, USA*

**Abstract.** The production of isolated single wall carbon nanotubes (SWNTs) is accomplished using the laser oven process. Material is collected on quartz substrates at different locations in the laser oven for a variety of flow conditions. The lengths and diameter distributions of the nanotubes are measured directly (without additional processing steps) using AFM. Preliminary Raman data taken using 2D scans indicate the feasibility of this technique for length and diameter determination. The AFM study indicated the formation of long individual nanotubes, which then seem to coalesce into bigger bundles. The role of the inner tube of the flow-tube set up is confirmed to improve interactions between SWNTs resulting in formation of bundles. Flowing buffer gas seems to influence the dispersion of particulate material in the nanotube product.

## INTRODUCTION

Carbon nanotubes are normally found as ropes/bundles of single wall or multiwall tubes. Most of the current work is on single wall nanotubes (SWNTs) because of their superior thermal, mechanical and electrical properties compared to multiwall nanotubes (MWNTs), resulting in many possible applications [1-3]. For the development of composite materials that can be reinforced mechanically by the nanotubes, issues of critical length and aspect ratio are important. Recent calculations [4] indicate that the lengths of the individual SWNTs need to be more than 10 μm in order to transfer individual tube strength to a bundle. Bundles have to be separated in order to observe and measure individual tubes. Some researchers have tried to infer the lengths of nanotubes by chromatographic methods [5], AFM and from scattering methods [6]. These results show tubes that may be too short after processing to be useful in composites. However, a recent measurement of tensile strength seems to indicate longer tubes [7]. It is therefore important to determine if the nanotubes are inherently long when they are produced and whether they get shorter during purification and processing. In order to be able to look at pristine SWNTs, “witness plates” (optical quality quartz flats and microscope slides) are placed at different locations in the laser oven. The roughness of such substrates is worse than normally used mica or silicon, but still adequate, and nanotubes bind well enough to allow AFM imaging.

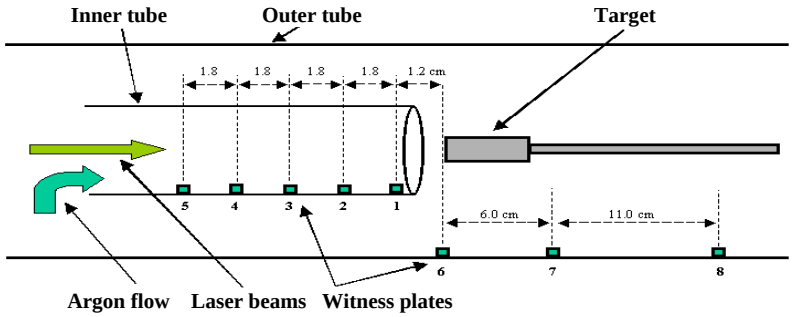


**FIGURE 1**. Lay out of the setup (double-pulse laser oven production process at 1473K with argon flowing at 500 Torr) for SWNT deposition directly on quartz flats that can be used as AFM substrates.

## EXPERIMENTAL DETAILS

The experiments are carried out in our pulsed laser vaporization setup, which is described in an earlier communication [8]. Eight witness plates are placed as shown in Fig. 1. Once the laser furnace is running, the laser beam shutters are opened briefly (0.5 sec) to deposit nanotubes onto the plates. Similar tests are conducted under run conditions with the gas flow stopped and without the inner tube to evaluate the effect of fluid flow changes and confinement of the plume. Plates are imaged in Digital Instruments Nanoscope IIIa, operating in the tapping mode. The height resolution is about 0.1 nm and we could image individual nanotubes and ropes. Raman spectra from these witness plates are obtained on a microprobe stage (2μ laser spot of 782 nm) of a Renishaw spectrometer using 2D scans with 0.5 μ step size.

## RESULTS AND DISCUSSION

### AFM Data

Production runs at 1473 K have produced some nanotubes close to the target (plates

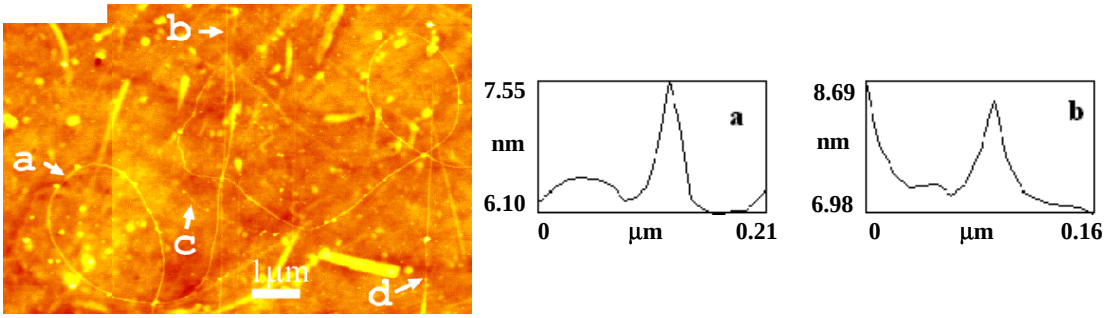


**FIGURE 2.** AFM image and corresponding height profiles of plate #3 exposed for 0.5 seconds, without inner tube and argon flowing at 100 sccm. a) Individual tube, 1.25 nm diameter and >22 μm long. b) Individual tube, 0.86 nm diameter, >18 μm long. c) Short tube, 0.8 nm diameter, 0.38 μm long. d) Tapered bundle.

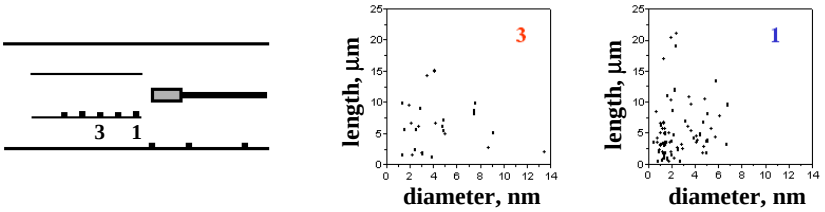


**FIGURE 3**. Diameter and length distributions of as prepared SWNTs on quartz substrates inside the laser oven at two different distances from the target. Notice shift towards more individual nanotubes and smaller diameter bundles closer to the target (1).

# 1, 2 and 3 with the inner tube and plates #3, 4 and 5 without the inner tube) and almost nothing on the rest of the witness plates (Fig. 2). Statistics on lengths and diameters obtained from AFM measurements is presented in Figure 3. It is important to emphasize that most length measurements are lower estimates, and nanotubes are definitely longer.

Far from the target we see almost exclusively bundles, while close to the target we see a significant fraction of individual tubes, and the bundles are generally much thinner (Fig. 3). This shows that nanotubes form within the ablation plume and propagate away from the target as it expands. As they fly away, they collide with each other and form bundles; hence more bundles and thicker bundles are found farther away from the target. Relative numbers of individual nanotubes vs. bundles deposited on the plates is always higher in experiments without the inner tube. In the presence of the inner tube, the volume into which the plume expands is smaller. Therefore the number density of nanotubes is higher, increasing the likelihood of tubes colliding with each other and forming bundles. Thus more and thicker bundles are produced with the inner tube.

Running at 1473 K with stopped flow produced too many particles on substrates to allow AFM imaging; nevertheless, nanotubes and bundles were seen in about the same abundance as in experiments with flow. Effective area of the nanotube greatly exceeds that of the nanoparticle of comparable weight, so they must move differently in the gas flow.

## Raman Data

Figure 4 displays a 2D Raman image of a 5 μ x 5 μ area on the plate # 1 (with inner

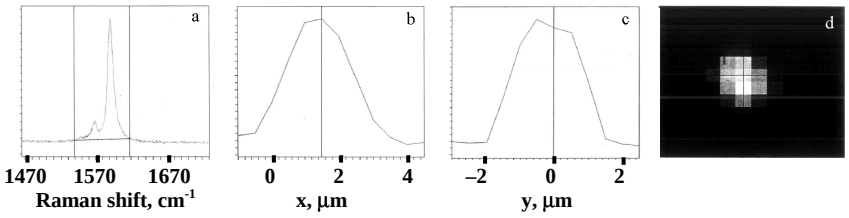


**FIGURE 4.** a) Tangential Raman mode of SWNT on plate #1. Indicated area under the peak was used for mapping. b, c) Raman signal profiles along X and Y axes. d) Raman intensity map of the 5 μm x 5 μm area.

tube). The image maps Raman intensity (area under the peak) of the 1590 $cm^{-1}$ SWNT line in 0.5 μ steps. Raman intensity distribution clearly indicates an isolated nanotube less than 2 μm in size (experimental resolution). The signal is surprisingly strong for such a small sample thus conforming the importance of resonant mechanism of Raman scattering from SWNTs. We note that the Raman image does not correlate with any of the AFM scans shown here. Nevertheless it demonstrates the potential of 2D Raman scans for detection of isolated SWNTs (ropes), in particular with length larger than the laser spot size.

## CONCLUSIONS

In conclusion, the current measurements indicate the formation of long individual nanotubes and their coalescence into ropes. The role of the inner tube is confirmed to control the expansion of the ablated plume and help their coalescence into bundles. The effect of argon flow seems to help distribute and dissipate bigger particulate material. Raman data indicates the need for improvement of 2D mapping by employing different excitation wavelengths and polarizations.

## ACKNOWLEDGMENTS

The authors wish to acknowledge helpful support and encouragement from Bob Hauge and Rick Smalley of Rice University.

## REFERENCES

1. Files, B. S. and Mayeaux, B. M., *Advanced Materials and Processes* **156**, 47-49 (1999).
2. Saito, R., Dresselhaus, G., and Dresselhaus, M. S., *Physical Properties of Carbon Nanotubes*, (Imperial College Press, London, 1998).
3. Dresselhaus, M. S., Dresselhaus, G., and Eklund, P. C., *Science of Fullerenes and Carbon Nanotubes* (Academic Press, San Diego, 1996).
4. Yakobson, B. I., Samsonidze, G. and Samsonidze, G. G., Carbon **38,** 1675-1680 (2000).
5. Duesberg, R. S., Muster, J., Krastic, V., Burghard, M. and Roth, S., *Applied Physics A* **67**, 117-120 (1998).
6. Liu, J., Rinzler, A. G., Dai, H., Hafner, J. H., Bradley, R. K., Boul, P. J., Lu, A., Iverson, T., Shelomov, K., Huffman, C. B., Rodriguez-Macias, F., Shon, Y-S., Lee, T. R., Colbert, D. L., and Smalley, R. E., *Science* **280**, 1253-1256 (1998).
7. Yu, M-F., Files, B.S., Arepalli, S. and Ruoff, R. S., *Physics Review Letters***, 84**, 5552-5555 (2000).
8. Arepalli, S., Nikolaev, P., Holmes, W., and Scott, C. D., *Applied Physics A* **70,** 125-133(2000).